Anion templated assembly of an indolocarbazole containing pseudorotaxane on beads and silica nanoparticles†

Liyun Zhao, Kathleen M. Mullen, Michał J. Chmielewski, Asha Brown, Nick Bampos, Paul D. Beer* and Jason J. Davis*

Received (in Durham, UK) 24th October 2008, Accepted 2nd December 2008
First published as an Advance Article on the web 14th January 2009
DOI: 10.1039/b818854h

The surface covalent attachment of fluorescent axles of indolocarbazole enables anion templation to be exploited in the formation of pseudorotaxane assemblies *via* the threading of neutral isophthalamide macrocycles. In utilising the surface of polystyrene beads this threading process can be followed by both magnetic resonance methods and changes in the axle fluorescent emission spectrum. The analogous surface assembly and anion templated threading can be achieved, with fluoride and sulfate, on silica nanoparticles where anion recognition and macrocycle threading are associated with equivalent and specific optical change.

Introduction

The prospect of utilising triggered molecular motion in sensing, data storage or machine-type applications has stimulated a great deal of interest in the synthesis and characterisation of interpenetrated and interlocked structures such as pseudorotaxanes, rotaxanes and catenanes. Though solution phase analyses have resolved cation, pH, redox and light triggered molecular motion,[1–11] it is the controlled interfacing of these molecules with solid electroactive or optically transparent surfaces that will lie central to many proposed applications. From a host–guest sensing perspective the advantages of tethering to a transducing interface, such as that presented by an electrode or optically transparent surface, are also considerable. In addition to the possibility of generating a robust and renewable host surface capable of operation in a variety of fluid media (static or flowing) there exists considerable evidence that the thermodynamics of host–guest association are favoured at such interfaces.[12,13] Although there have been several reported examples of the covalent attachment of interlocked molecular systems to solid surfaces,[14–24] in comparatively few instances has surface assembly been well-defined. One of the most highly investigated classes of supramolecular systems is the rotaxanes and pseudorotaxanes. While the surface assembly of these has been achieved using intermolecular forces between neutral species[20] or cationic species,[19,25] employing anions to template the formation of surface confined interpenetrated structures has only recently been investigated.[26,27]

The incorporation of the indole motif into anion receptors is a recent development in the field of anion recognition. The strong binding affinities and high anion selectivity of the indole- and biindole motif has, in particular, been used by the groups of Beer, Jeong, Pfeffer, Jurczak, Sessler and Gale.[27–42] With the aim of using anions to template the formation of interpenetrated and interlocked structures,[43] indolo[2,3-*a*]carbazoles are attractive anion receptors due to both their rod-like shape and their preorganised hydrogen bond donating pyrrole groups which have been shown to bind anions strongly.[29,30,32,37] We have recently reported the unprecedented anion templation of a neutral pseudorotaxane assembly using an indolocarbazole threading component.[27] Indeed threading of the indolocarbazole component through the annulus of an isophthalamide containing macrocycle is only observed upon the addition of either the doubly charged sulfate anion, or fluoride. Furthermore we have demonstrated analogous anion templated pseudorotaxane assembly on gold surfaces as monitored by SPR.[27]

Towards the ultimate goal of fabricating fluorescent anion responsive interlocked host functionalised receptors we report herein the TentaGel polystyrene bead and silica nanoparticle surface immobilisation of indolocarbazole axles together with anion association and templated pseudorotaxane formation with a charge neutral isophthalamide macrocycle (see Fig. 1). Though surface spectroscopic (and electroanalytical) methods can be powerfully applied to the characterisation of surface

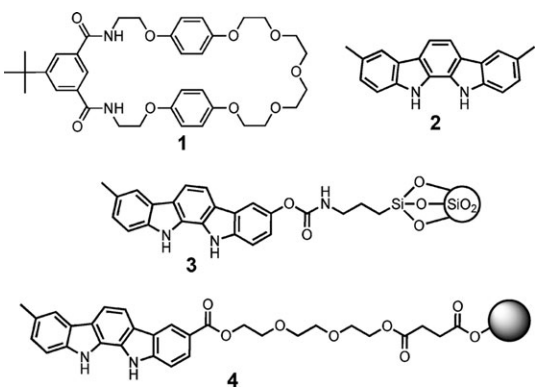

Fig. 1 Structure of isophthalamide macrocycle **1**, model indolocarbazole compound **2**, silica nanoparticle tethered indolocarbazole **3**, and polystyrene bead tethered indolocarbazole **4**.

Chemistry Research Laboratory, University of Oxford, Mansfield Road, Oxford, UK OX1 3TA. E-mail: paul.beer@chem.ox.ac.uk. E-mail: jason.davis@chem.ox.ac.uk

† Electronic supplementary information (ESI) available: FTIR of **3**, ^{1}H NMR titration spectra of **4** and **13**. See DOI: 10.1039/b818854h

confined molecules, they are not, generally, capable of providing information as "chemically-refined" as that offered by magnetic resonance (the latter having now been extensively applied to the analysis of structural and dynamic characteristics of interlocked systems in solution). To bridge this gap and confirm the presence of anion templated and particle surface confined pseudorotaxanes we have used herein high resolution magic angle spinning (HR MAS) ^{1}H NMR on molecules tethered to swollen polymer resin beads (facilitating access to data gathered routinely in solution).[44–51] For both particle types anion association and templated threading is additionally monitored through perturbations in the indolocarbazole axle fluorescence emission spectrum.[52]

Results and discussion

Synthesis

The indolocarbazole silica nanoparticles **3** and indolocarbazole functionalised polystyrene beads **4** as shown in Fig. 1, were synthesised according to Scheme 1 and 2. Triethoxysilyl-terminated indolocarbazole derivatives suitable for tethering to silica nanoparticle surfaces were prepared as shown in Scheme 1. Methyl ether functionalised indolocarbazole **6** was prepared according to literature procedures *via* stepwise Fisher indolisation of cyclohexane-1,2-dione with *p*-tolylhydrazine followed by reaction with 4-methoxyphenylhydrazine hydrochloride.[27] Demethylation of **6** was achieved using BBr_3 to give mono-hydroxy indolocarbazole derivative **7**. Reaction of **7** with 3-(triethoxysilyl)propyl isocyanate in THF afforded the triethoxylsilane tethered indolocarbazole **8** in quantitative yield. Confinement of **8** on silica nanoparticles was obtained by refluxing commercially available silica nanoparticles with freshly prepared **8** in THF (in an amount designed to provide a well-dispersed particle coverage—see below). Functionalised nanoparticles **3** were repeatedly washed and centrifuged with THF, the covalent attachment of **8** being confirmed by FTIR and fluorescence spectroscopy

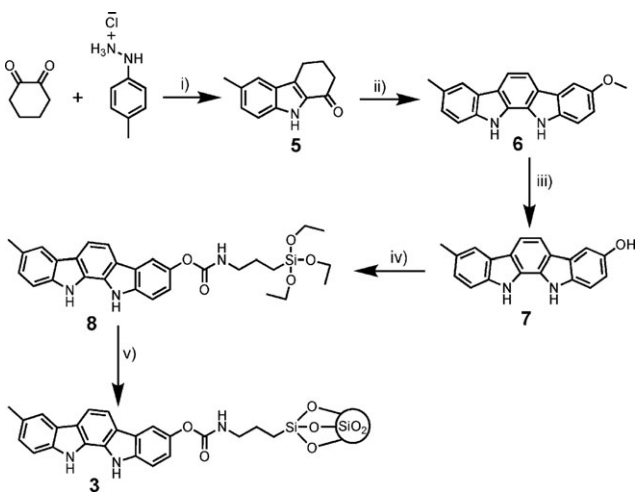

Scheme 1 Synthesis of indolo[2,3-*a*]carbazole silica nanoparticles **3**; (i) H_2SO_4, EtOH, reflux, 16 h, 39%; (ii) 4-methoxyphenylhydrazine hydrochloride, H_2SO_4, *n*-BuOH, 90 °C, 24 h, 48%; (iii) BBr_3, CH_2Cl_2, −78 °C 1 h, to r.t. 16 h, 85%; (iv) 3-(triethoxysilyl)propyl isocyanate, Et_3N, THF, reflux, 48 h, 98%; (v) silica nanoparticles, THF, reflux, 24 h.

(the emission spectrum of the particle solution bearing the indolocarbazole fingerprint and the formation of Si–O–Si bonds on the particle surface being detectable by FTIR—see Fig. S1, ESI†). Model compound **2** was also synthesised according to literature procedures for comparative solution phase titration experiments.[37]

Carboxyl-terminated indolocarbazole derivatives suitable for tethering to polystyrene bead surfaces were prepared using the synthetic pathway shown in Scheme 2. Unsymmetrically functionalised indolocarbazole **9** was synthesised from a one-pot Fisher indolisation of cyclohexane-1,2-dione with 4-hydrazinylbenzoic acid and *p*-tolylhydrazine. Ester hydrolysis afforded indolocarbazole **10**. Microwave irradiation of **10**, 2-(2-(2-chloroethoxy)ethoxy)ethanol, and Cs_2CO_3 in dry DMF, gave the polyethylene glycol substituted indolocarbazole **11**. This was converted to the acid derivative **12** *via* reaction with succinic anhydride and attached to TentaGel HL-OH polystyrene beads using literature procedures (with a 20 fold excess of the calculated maximum possible bead loading reported to be 0.40 mmol g^{-1} by the manufacturer).[53,54] Although a variety of similar polystyrene resins with various functionality are now commercially available, TentaGel-OH beads, with terminal alcohol groups, were selected to tether the indolocarbazole thread as these have been previously used successfully in HR MAS NMR experiments.[53] The loading of the indolocarbazole tethered beads **4** was calculated by elemental analysis to be 0.21 mmol g^{-1}, which is approximately 53% of the estimated functional group loading (0.40 mmol g^{-1}) reported by the manufacturer. This surface coverage has been shown to be sufficient in order to obtain good quality ^{1}H spectra using HR MAS NMR.[54] **12** was also converted to its methyl ester **13** to provide a model compound for comparative solution NMR experiments.

NMR investigations

We have previously reported the anion templated pseudorotaxane assembly between an isophthalamide macrocycle **1** and indolocarbazole in d_3-acetonitrile solution.[27] In the absence of sulfate (or fluoride) no evidence of pseudorotaxane assembly is observed by ^{1}H NMR. However when TBA sulfate is added to a 1 : 1 solution of macrocycle **1** and indolocarbazole the macrocycle hydroquinone protons are observed to shift significantly upfield, which is indicative of interpenetration. In extending this work to surfaces one would normally not retain access to structural and dynamic information available in solution. The use of high resolution magic angle spinning (HR MAS) NMR on systems covalently attached to swollen polymer resin beads (such as TentaGel-OH), however, allows the possibility of obtaining NMR spectra comparable to solution state spectra.[44,45,48–51] Hence direct comparison can be made between solution and solid-tethered self-assembly and dynamics of complex supramolecular systems. Thus in an effort to bridge this gap HR MAS ^{1}H NMR studies of polystyrene tethered indolocarbazole beads **4** were performed.

The HR MAS ^{1}H NMR spectrum in d_3-acetonitrile of the indolocarbazole tethered beads **4** indicated successful attachment of the thread to the polystyrene beads with resonances for the indolocarbazole NH protons evident at

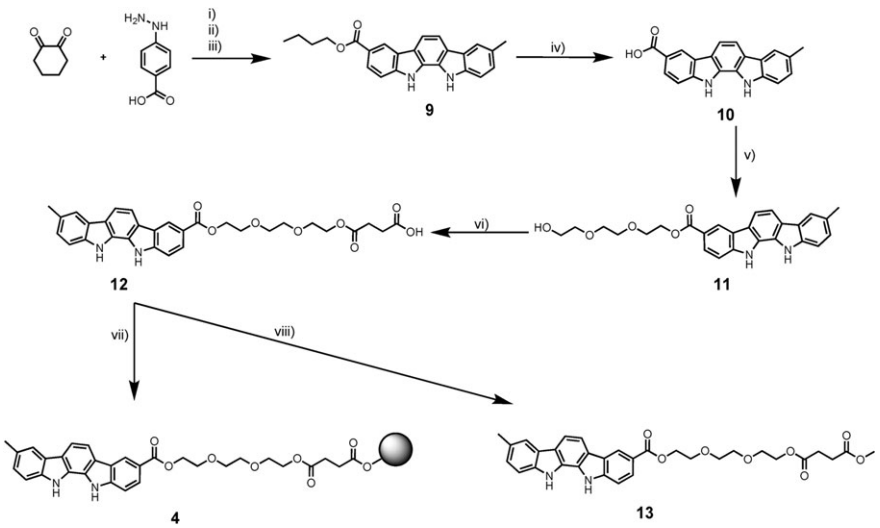

Scheme 2 Synthesis of polystyrene bead tethered indolo[2,3-*a*]carbazole **4**; (i) H_2SO_4, BuOH, 90 °C, 4 h; (ii) *p*-tolylhydrazine, 90 °C, 24 h; (iii) Pd/C, DMF, reflux, 24 h, 68%; (iv) KOH, *i*-PrOH–H_2O, reflux, 36 h, 72%; (v) 2-(2-(2-chloroethoxy)ethoxy)ethanol, K_2CO_3, 140 °C, 1 h, 41%; (vi) succinic anhydride, DMAP, Et_3N, r.t, 18 h, 74%; (vii) tentagel-OH beads, EDAC, HOBt, Et_3N, THF–CH_2Cl_2, r.t, 10 days; (viii) EDAC, DMAP, MeOH–CH_2Cl_2, r.t, 18 h, 93%.

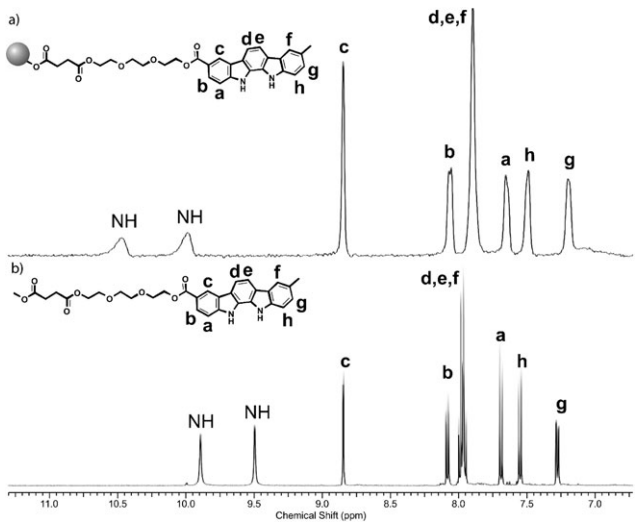

Fig. 2 Direct NMR comparison between solution phase and solid bound indolocarbazole threads: top spectrum – HR MAS ^{1}H NMR spectrum of TentaGel™-OH bound indolocarbazole **4** in CD_3CN; bottom spectrum – ^{1}H NMR spectrum of indolocarbazole **13** (3 mM) in CD_3CN.

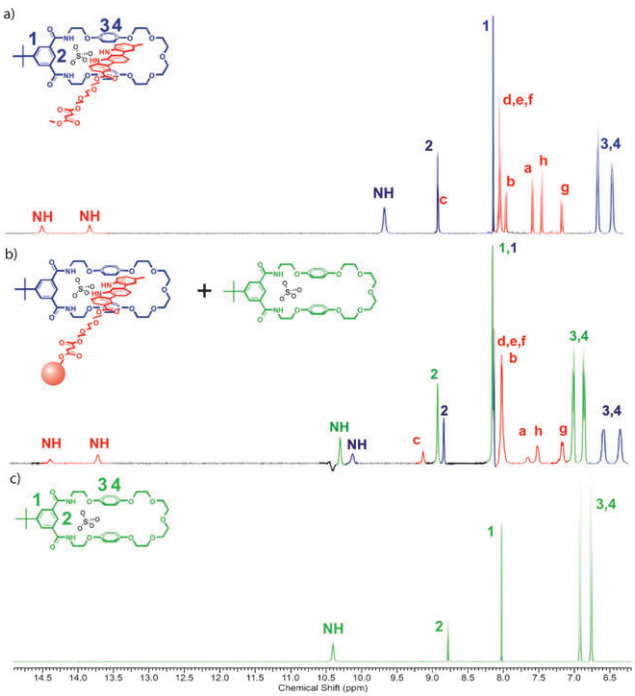

Fig. 3 (a) ^{1}H NMR spectrum of a 1 : 1 : 1 mixture of indolocarbazole **13**, macrocycle **1** and $(TBA)_2SO_4$ in CD_3CN, (b) HR MAS NMR spectrum of TentaGel™-OH bound indolocarbazole **4** in the presence of excess macrocycle **1** and $(TBA)_2SO_4$ in CD_3CN, (c) ^{1}H NMR spectrum of a 1 : 1 mixture of macrocycle **1** and $(TBA)_2SO_4$ (both 3 mM) in CD_3CN.

10.48 and 9.99 ppm with additional indolocarbazole proton peaks at 8.85, 8.07, 7.90, 7.66, 7.49, 7.20 ppm (Fig. 2). Slight downfield shifts in the NH protons for the bead tethered system when compared directly to the ^{1}H NMR spectrum of the solution analogue **13** were observed. Addition of an excess of $(TBA)_2SO_4$ to the Tentagel-bound indolocarbazole in CD_3CN produced large (~4 ppm) downfield shifts in the indolocarbazole NH proton resonances due to strong hydrogen bonding with the sulfate anion. Though accurately quantified binding constants cannot be generated, the extent of this NH proton shift is both consistent with that seen in analogous solution studies, and indicative of non-compromised anion binding at the solid surface (see Fig. S2, ESI†). Under similar concentration conditions, an equimolar solution of macrocycle **1** and TBA sulfate was then added to the indolocarbazole tethered beads. The NH peaks again were observed to have shifted significantly downfield (to 14.29 and 13.61 ppm, respectively), though to a slightly lesser extent than that observed for systems containing only TBA sulfate in the absence of macrocycle (Fig. 3). Similar shifts are observed in

analogous solution studies (see Fig. S3, ESI†) and attributed to a weakening of the anion–indolocarbazole hydrogen bonds due to macrocycle binding *i.e.*, are indicative of pseudorotaxane formation. More conclusive evidence of pseudorotaxane formation arises from the fact that two distinct sets of macrocycle proton resonances were evident (Fig. 3b). The more downfield (green) set of protons displayed an NH peak at 10.20, and hydroquinone peaks at 6.90 and 6.77 ppm. Direct comparison with the analogous solution studies suggests that this species corresponds to a 1 : 1 macrocycle–$(TBA)_2SO_4$ complex (Fig. 3c). The other (more upfield) set of macrocycle protons (blue) has a NH peak at 10.03, and hydroquinone peaks at 6.47 and 6.25 ppm. In solution studies we have shown that upfield shifts in the macrocycle hydroquinone protons are indicative of the formation of interpenetrated structures.[27] Furthermore direct comparison with analogous solution studies indicate that the chemical shifts of these protons are consistent with a pseudorotaxane 1 : 1 : 1 macrocycle–indolocarbazole–$(TBA)_2SO_4$ structure (Fig. 3b), thus confirming that anion induced threading of solid surfaces is possible.

Contrary to solution experiments, these results suggest that the pseudorotaxane formation on the bead surface is in slow exchange on the chemical shift timescale. Given the diffusive restrictions present at even a highly curved interface, this is not surprising. However, it is possible that the downfield set of macrocycle resonances (green) originates from molecules physically 'entangled' in the bead core (and thus unable to access the indolocarbazole thread) as has been observed in other systems.[53] Though further elucidation of this would require detailed variable temperature analyses, results herein confirm that sulfate templated pseudorotaxane formation on the surface of the polystyrene beads is occurring, regardless of whether the dynamics are in fast or slow exchange.

Fluorescence investigations

Previous work has demonstrated the indolocarbazole hydrogen bonding association with anions can be followed by fluorescence modulation of the host.[52] Consistent with this, the addition of TBA sulfate to an acetonitrile solution of **2** was observed to lead to a loss of emission at 370 and 387 nm and an increase at 405 nm. The subsequent addition of a molar equivalent of macrocycle **1** to **2** and TBA sulfate leads to further perturbation of the emission spectrum (Fig. 4). These changes, which are not observed on the addition of macrocycle to **2** in the absence of anion, are ascribed to macrocycle threading over the indolocarbazole axle hydrogen bonded to the templating anion. These observations are, additionally, anion specific; analogous threading induced emission changes are observed with fluoride but not with chloride or hydrogen sulfate, fully consistent with the reduced hydrogen bonding affinity of these anions as evidenced from ^{1}H NMR titrations (Fig. 5).[27]

Silica nanoparticles are diffusively mobile, non-quenching, optically transparent and lend themselves to solution phase optical switching or optical detection applications that

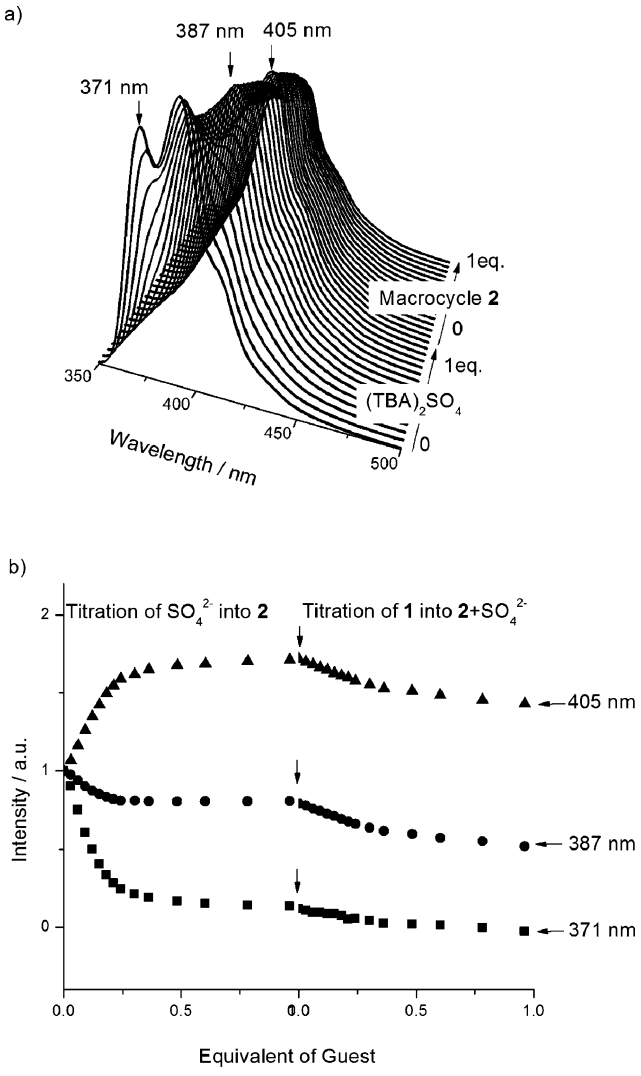

Fig. 4 (a) Sequential fluorescence titration spectra showing the effects of adding a molar equivalent of sulfate followed by macrocycle **1** into an acetonitrile solution of compound **2** (4.2×10^{-5} mol L^{-1}) and (b) plotted emission changes at 371, 387 and 405 nm (as arrow indicated).

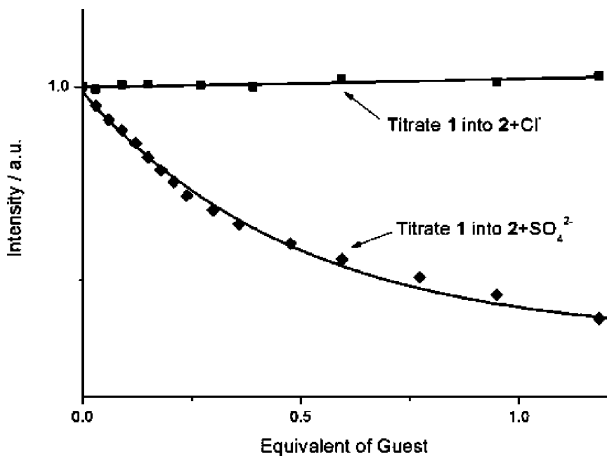

Fig. 5 Fluorescence titration plots (scattered) and associated fitting curves (solid) of emission changes in axle **2** on the addition of macrocycle **1** in the presence of different anions. Significant emission intensity changes are observed with sulfate but not with chloride (titrations in acetonitrile, 4.2×10^{-5} mol L^{-1} in **2**). Excitation 330 nm; emission 387 nm.

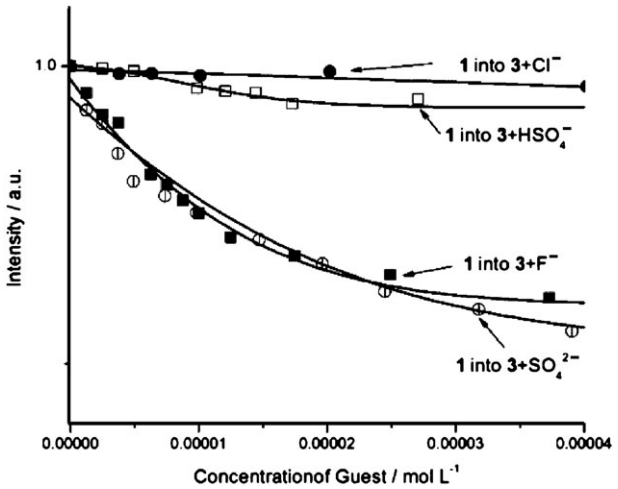

Fig. 6 Fluorescence titration curves (scattered) and associated fitting curves (solid) of macrocycle **1** addition to acetonitrile solutions of indolocarbazole modified silicate nanoparticles **3** in the presence of different anions. Significant emission intensity decreases are observed for SO_4^{2-} and F^- but not for Cl^- or HSO_4^-. Excitation: 330 nm; emission: 387 nm.

encompass the advantages of receptor surface immobilisation. This transparency facilitates an equivalent optical analysis of anion association with surface confined indolocarbazole moieties and their subsequent templated threading (Fig. 6 and 7). The addition of sulfate to functionalised nanoparticle solutions leads to fluorescence intensity decrease and 6 nm bathochromic shift in the two resolved emission maxima. Subsequent addition of **1** leads to further decrease in emission with no further spectral shift. In assuming that the surface hydroxyl group density is not limiting in the silane condensation efficacy and that the reaction goes to completion, the footprint of the axle can be estimated from $F_p = \frac{M_I \times A_S \times W_S}{W_I \times N_A}$ where A_S is the surface area of silica nanoparticles (manufacturers value 590–690 $m^2\ g^{-1}$), M_I is the molecular weight of **8**, N_A is Avogadro's number, and W_I and W_S are the mass of **8** and silica nanoparticles as reactant, respectively. The derived value of 26–30 nm^2 (indicative of a low packing density; this is both consistent with the axle emission spectrum being the same as that observed in solution and facilitates threading) can be used to estimate the relative concentrations of axle and anion in solution phase titrations. The titration curves shown in Fig. 6 show the macrocycle induced axle emission change in the presence of different anions. Significant changes are observed with sulfate and fluoride but not chloride or hydrogen sulfate consistent with the ability of only the former to template threading. Though anion and macrocycle are present in a 1 : 1 molar equivalence to each other, spectral changes in surface confined **2** continue to be observed at several molar equivalents to the axle (presumably reflecting a kinetic barrier associated with accessing the surface constrained axle). The fact that the same anion selectivity for these changes is maintained as observed for **2** in solution or bead mounted **4** (in that macrocycle induced axle emission changes are observed only in the presence of fluoride and sulfate, Fig. 6) strongly supports the occurrence of template threading at the nanoparticle surface.

Though spectral quality was limited by particle scattering, axle derivatised beads **4** (suspended in solution) exhibited optical responses to sulfate and macrocycle **1** consistent with that observed in solution with the free axle. A comparison of sequential titration results of systems **2**, **3**, and **4** in acetonitrile is displayed in Fig. 7. In all cases, the initial hydrogen bonding association of sulfate leads to emission intensity decrease and a 5–6 nm bathochromic shift. Subsequent addition of macrocycle **1** leads to further emission decrease with no associated spectral shift. It is noteworthy that these observations are not made unless both sulfate and macrocycle are present in solution.

Conclusion

Despite the highly tuneable optical and electrical characteristics potentially offered, there have been only a few published studies in which a synthesised interlocked structure has been

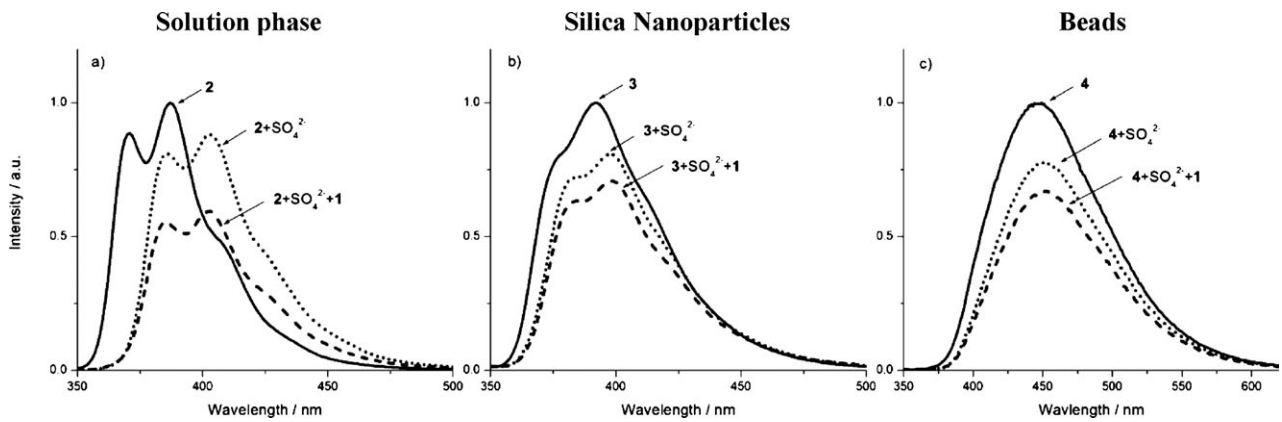

Fig. 7 Fluorescence spectra of (a) **2** (solid curve) in acetonitrile (4.2×10^{-5} mol L^{-1}) and on the sequential addition of 1 molar equivalence of sulfate (dotted curve) and macrocycle **1** (dashed curve); (b) silica nanoparticle surface confined indolocarbazole **3** (solid curve) in acetonitrile (0.05 wt%) and the results of sequential addition of sulfate (dotted curve) and macrocycle **1** (dashed curve), respectively; and (c) polystyrene beads confined indolocarbazole **4** (solid curve) and its sequential addition of sulfate (dotted curve) and macrocycle **1** (dashed curve), respectively. Initial peak shape and wavelength differences for **2**, **3** and **4** in the absence of anions and macrocycles are attributed to the combined effects of different conformational freedom/aggregation states of the emitter.

assembled on a nanoparticle surface. In the first example, Fitzmaurice and co-workers described the assembly of a hetero[2]pseudorotaxane and an electrochemically addressable and switchable hetero[2]rotaxane on titanium dioxide nanoparticles through the attachment of a tripodal phosphonate unit.[21,55] Stoddart and co-workers have subsequently reported the establishment of a series of "nanovalves" on silica nanoparticles from redox or pH driven motion in assembled bistable [2]pseudorotaxanes. These units are demonstrably capable of functioning as gatekeepers for the controlled release of dye molecules from the underlying porous silica nanoparticle.[23,24,56] Silica nanoparticles are readily prepared by the controlled polymerisation of silane precursors under a variety of solution phase conditions. Highly monodisperse preparations are now accessible and can be doped with a variety of imaging agents.[57–60] In most preparations the surface of these particles remain accessible to subsequent robust modification with dyes, biomolecules or host–guest receptors.[61–66] We have demonstrated here the nanoparticle surface assembly of hydrogen bonding indolocarbazole axles. The subsequent specific anion templated threading of an appropriate charge neutral macrocycle over these can be monitored spectroscopically. These fluorescence observations mirror those made on swollen polymer beads where HR MAS NMR analysis has further confirmed pseudorotaxane formation. The nature of the anion dictates whether surface pseudorotaxane assembly is successful, where fluoride and sulfate are effective whilst chloride and hydrogen sulfate are not, paralleling observations made in solution.

Experimental

General considerations

Dry solvents were obtained by purging with nitrogen and then passing through an MBraun MPSP-800 column. H_2O was de-ionised and microfiltered using a Milli-Q® Millipore machine. Tetrabutylammonium sulfate was purchased from Sigma-Aldrich as a 50% aqueous solution, which was concentrated on a rotary evaporator and subsequently dehydrated by azeotroping with tetrahydrofuran and then dried over phosphorus pentoxide in a vacuum desiccator. All tetrabutylammonium salts were stored in a vacuum desiccator over phosphorus pentoxide prior to use. All other solvents and commercial grade reagents were used without further purification.

Solution ^{1}H and ^{13}C NMR spectra were recorded on a Varian Mercury-VX 300, a Varian Unity Plus 500 or a Bruker AVII500 with cryoprobe at 293 K. HR MAS NMR spectra were acquired on a Bruker DRX400 spectrometer at room temperature using a Bruker HR MAS probe. Rotors containing a suspension of the beads in $CDCN_3$ were spun at 4 kHz. One-dimensional HR MAS spectra were obtained with 64 scans. CPMG pulse sequence contained 32 or 2000 π-pulses with a repetition time of 30 ms. Chemical shifts (δ) are reported in parts per million relative to residual solvent. J values are given in Hz. Mass spectra were obtained using a Micromass GCT (EI) instrument or a Micromass LCT (ESMS) instrument. Microwave reactions were carried out using a Biotage Initiator 2.0 microwave. Melting points were recorded on a Gallenkamp capillary melting point apparatus and are uncorrected. 6-Methyl-2,3,4,9-tetrahydro-1*H*-carbazol-1-one **5**,[27] 3-methoxy-8-methyl-11,12-dihydroindolo[2,3-*a*]-carbazole **6**,[27] 8-methyl-11,12-dihydroindolo[2,3-*a*]carbazol-3-ol **7**,[27] 3,8-dimethyl-11,12-dihydroindolo[2,3-*a*]carbazole **2**,[52] and isophthalamide macrocycle **1** were prepared as described previously.[67] FTIR spectra were recorded using a Varian Digilab FTS 7000 series FTIR spectrometer, with a DurasamplIR II diamond attenuated total reflectance (ATR) accessory. Fluorescence spectra were recorded on a Hitachi F-4500 Fluorescence Spectrometer (excitation wavelength set at 330 nm). Solution phase sequential titration protocol: (1) sulfate added until 1 molar equivalence into acetonitrile solution of **2** (4.2×10^{-5} mol L^{-1}); (2) macrocycle added until 1 molar equivalence into 1 : 1 molar equivalence of indolocarbazole–sulfate in acetonitrile. Particle confined systems titration protocols are as follows: (1) sulfate added to acetonitrile suspension of particle confined indolocarbazole until emission stabilises; (2) macrocycle added until 1 molar equivalence to total sulfate into particle confined indolocarbazole–sulfate suspension.

8-Methyl-11,12-dihydroindolo[2,3-*a*]carbazol-3-yl 3-(triethoxysilyl)propylcarbamate 8

3-Hydroxy-8-methyl-11,12-dihydroindolo[2,3-*a*]carbazole **7** (65 mg, 0.23 mmol) and 3-(triethoxysilyl)propyl isocyanate (60 μL, 0.23 mmol) were suspended in dry THF (10 ml) under N_2. Et_3N (60 μL) was then added and the mixture was refluxed under N_2 for 48 h. After this time, solvent and excess Et_3N were removed by rotary evaporation and the product was dried under high vacuum to give an off-white solid in quantitative yield which was used immediately without further purification; δ_H (300 MHz, DMSO-d_6) 11.01 (1 H, s, N*H*), 10.92 (1 H, s, N*H*), 7.91 (1 H, s, Ar*H*), 7.82 (1 H, d, J 0.1, Ar*H*), 7.82 (1 H, s, Ar*H*), 7.81 (1 H, d, J 5.5, Ar*H*), 7.71 (1 H, t, J 5.1, N*H*), 7.61 (1 H, d, J 8.7, Ar*H*), 7.54 (1 H, d, J 8.4, Ar*H*), 7.18 (1 H, d, J 8.0, Ar*H*), 7.05 (1 H, dd, J 8.7 and 2.0, Ar*H*), 3.71 (6 H, q, J 6.1, CH_2), 2.90 (2 H, m, CH_2), 2.48 (3 H, s, CH_3, coincident with DMSO), 1.37 (2 H, m, CH_2), 1.12 (9 H, t, J 7.9, CH_3), 0.47 (2 H, t, J 7.9, CH_2); m/z (EI) 533.2 (M^+, $C_{29}H_{35}N_3O_5Si$ requires 533.2).

Synthesis of indolo[2,3]carbazole-functionalised silica nanoparticles 3

1 g of pre-dried silica nanoparticles (Aldrich, silica nanopowder, 10 nm, BET surface area 590–690 m^2 g^{-1}) were suspended in 50 ml dry THF under N_2. Freshly prepared 8-methyl-11,12-dihydroindolo[2,3-*a*]carbazol-3-yl 3-(triethoxysilyl)propylcarbamate **8** (20 mg, 0.07 mmol) was added and the mixture was refluxed for 24 h. The obtained functionalised nanoparticles were repeatedly washed and centrifuged with THF until there was no fluorescence signal in the supernatant. The nanoparticles were then dried under high vacuum and stored in a glove box.

Butyl 8-methyl-11,12-dihydroindolo[2,3-*a*]carbazole-3-carboxylate 9

p-Hydrazinebenzoic acid (0.76 g, 5.0 mmol) and 1,2-cyclohexanedione (0.56 g, 5.0 mmol) were dissolved in *n*-butanol (20 mL). Concentrated H_2SO_4 (1 mL) was then added dropwise *via* syringe. The solution was heated to 90 °C for 4 h, after which time *p*-tolylhydrazine (0.95 g, 6.0 mmol) was added as a solid. After being heated to 90 °C for a further 24 h, the reaction mixture was cooled to room temperature and then allowed to stand at 4 °C for 16 h. The resulting precipitate was collected by filtration and washed with H_2O (100 mL), MeOH (3 × 10 mL) and CH_2Cl_2 (2 × 10 mL). The pale yellow solid was then dissolved in DMF (20 mL) and 10% Pd/C (0.125 g, ~10% by weight) was added. The reaction mixture was refluxed under N_2 for 24 h. After this time the solution was filtered to remove the catalyst, which was washed with hot DMF (5 mL). The filtrate and DMF washings were combined and diluted with H_2O (100 mL), upon which a white precipitate formed. This was collected by filtration, washed with H_2O (8 × 30 mL) followed by MeOH (3 × 10 mL) and dried under high vacuum to afford the product (1.261 g, 68%) as a white solid; mp 275 °C (decomp.); δ_H (300 MHz; DMSO-d_6) 11.53 (1 H, s, N*H*), 11.01 (1 H, s, N*H*), 8.80 (1 H, d, *J* 1.5, Ar*H*), 8.01 (1 H, dd, *J* 8.7 and 1.5, Ar*H*), 8.0 (1 H, d, *J* 8.2, Ar*H*), 7.97 (1 H, br s, Ar*H*), 7.94 (1 H, d, *J* 8.2, Ar*H*), 7.77 (1 H, d, *J* 8.7, Ar*H*), 7.59 (1 H, d, *J* 8.2, Ar*H*), 7.23 (1 H, dd, *J* 8.2 and 1.5, Ar*H*), 4.33 (2 H, t, *J* 6.5, CO_2CH_2), 2.50 (3 H, CH_3 coincident with DMSO), 1.76 (2 H, m, CH_2), 1.49 (2 H, m, CH_2), 0.98 (2 H, t, *J* 7.3, CH_3); δ_C (125 MHz; DMSO-d_6) 166.6, 141.7, 137.4, 127.7, 126.3, 126.2, 125.8, 125.5, 123.8, 123.6, 121.7, 120.6, 120.5, 119.9, 119.6, 112.5, 111.5, 111.4, 64.0, 30.5, 21.2, 18.9, 13.7; *m*/*z* (EI) 370.19 (M^+, $C_{24}H_{22}N_2O_2$ requires 370.17).

8-Methyl-11,12-dihydroindolo[2,3-*a*]carbazole-3-carboxylic acid 10

Butyl 8-methyl-11,12-dihydroindolo[2,3-*a*]carbazole-3-carboxylate **9** (0.62 g, 1.7 mmol) was suspended in propan-2-ol (24 mL) and a solution of potassium hydroxide (6.0 g, 106 mmol) in H_2O (40 mL) was added. The mixture was heated to reflux under N_2 for 36 h until the starting material had dissolved. The reaction mixture was cooled to room temperature and acidified with 1 M $HCl_{(aq)}$. The resulting yellow precipitate was collected by filtration and washed thoroughly with H_2O (8 × 25 mL) followed by MeOH (2 × 15 mL) and CH_2Cl_2 (2 × 15 mL). After drying under high vacuum, the title compound was obtained as a white solid (0.40 g, 75%); mp > 300 °C; δ_H (300 MHz, DMSO-d_6) 12.56 (1 H, br s, CO_2H), 11.47 (1 H, s, N*H*), 10.98 (1 H, s, N*H*), 8.80 (1 H, s, Ar*H*), 8.05–8.02 (1 H, dd, *J* 8.5 and 1.2, Ar*H*), 7.99–7.90 (2H, m, Ar*H*), 7.75–7.73 (1 H, d, *J* 8.50, Ar*H*), 7.60–7.58 (1 H, d, *J* 8.5, Ar*H*), 7.24–7.22 (1 H, d, *J* 7.9, Ar*H*), 2.50 (1 H, CH_3, coincident with DMSO-d_6); δ_C (75 MHz; DMSO-d_6) 168.3, 141.6, 137.4, 127.7, 126.3, 126.2, 125.9, 125.8, 123.8, 123.6, 122.0, 121.4, 120.6, 120.0, 119.6, 112.5, 111.5, 111.4, 111.3, 21.2; *m*/*z* (EI) 314.1059 (M^+, $C_{20}H_{14}N_2O_2$ requires 314.1055).

2-(2-(2-Hydroxyethoxy)ethoxy)ethyl 8-methyl-11,12-dihydroindolo[2,3-*a*]carbazole-3-carboxylate 11

Dry, de-gassed DMF (10 mL) was added to a mixture of 8-methyl-11,12-dihydroindolo[2,3-*a*]carbazole-3-carboxylic acid **10** (0.20 g, 0.64 mmol) and K_2CO_3 (0.22 g, 0.64 mmol) in a microwave vial. The vial was sealed and 2-(2-(2-chloroethoxy)-ethoxy)ethanol (0.18 mL, 1.2 mmol) was added *via* syringe. The mixture was purged with N_2 for 10 minutes before being heated to 140 °C for 60 minutes using microwave irradiation. After cooling to room temperature the mixture was filtered and the precipitate was washed with DMF (2 × 10 mL). The combined filtrate and DMF washings were concentrated *in vacuo* to yield a viscous yellow oil. Addition of H_2O (100 mL) caused the product to precipitate as an oily white solid. This was collected by filtration through a plug of celite and the celite was washed with H_2O (4 × 20 mL). The product was then eluted from the celite by washing with CH_2Cl_2–MeOH 1 : 1 (~200 mL) until the filtrate contained no UV active material. The CH_2Cl_2–MeOH washings were concentrated *in vacuo* and the residual pale yellow oily solid was purified by column chromatography (SiO_2; 2% MeOH–CH_2Cl_2) to give the title compound (0.12 g, 41%) as a waxy white solid; mp 228–230 °C; δ_H (300 MHz, DMSO-d_6) 11.54 (s, 1 H, N*H*), 11.01 (s, 1 H, N*H*), 8.80 (1 H, d, *J* 1.3, Ar*H*), 8.02 (1 H, dd, *J* 8.2, and 1.3, Ar*H*), 7.99 (1 H, d, *J* 8.2, Ar*H*), 7.98 (1 H, br s, Ar*H*), 7.94 (1 H, d, *J* 8.2, Ar*H*), 7.77 (1 H, d, *J* 8.2, Ar*H*), 7.59 (1 H, d, *J* 8.2, Ar*H*), 7.23 (1 H, dd, *J* 8.21 and *J* 1.2) Ar*H*), 4.59 (1 H, t, *J* 5.6, O*H*), 4.44 (2 H, m, CH_2), 3.81 (2 H, m, CH_2), 3.67–3.63 (2 H, m, CH_2), 3.59–3.56 (3 H, m, CH_2), 3.49–3.44 (3 H, m, CH_2); δ_C (75 MHz, DMSO-d_6) 166.6, 141.8, 137.4, 127.7, 126.3, 126.2, 125.8, 125.6, 123.7, 123.6, 121.8, 120.7, 120.2, 119.9, 119.6, 112.6, 111.4, 72.4, 70.0, 69.8, 68.6, 63.7, 60.2, 21.2; *m*/*z* (ES) 469.1734 ($[M + Na]^+$, $C_{26}H_{26}N_2NaO_5$ requires 469.1734).

1-(8-Methyl-11,12-dihydroindolo[2,3-*a*]carbazol-3-yl)-1,12-dioxo-2,5,8,11-tetraoxapentadecan-15-oic acid 12

2-(2-(2-Hydroxyethoxy)ethoxy)ethyl 8-methyl-11,12-dihydroindolo[2,3-*a*]carbazole-3-carboxylate **11** (0.10 g, 0.22 mmol), succinic anhydride (0.067 g, 0.67 mmol) and 4-(dimethylamino)-pyridine (0.003 g, 0.025 mmol) were dissolved in dry DMF (3 mL). Distilled Et_3N (0.16 mL, 1.2 mmol) was added and the solution was stirred at room temperature under N_2 for 18 h. The reaction mixture was then diluted with CH_2Cl_2 (100 mL) and washed with 1 M $HCl_{(aq)}$ (3 × 50 mL), H_2O (2 × 75 mL) and brine (75 mL). The organic layer was evaporated to dryness. The residual yellow solid was dissolved in MeOH, dry-loaded onto silica and purified by column chromatography (SiO_2; 5% MeOH–EtOAc) to yield the product (0.091 g, 74%) as a pale yellow solid; mp 190 °C (decomp.); δ_H (300 MHz, DMSO-d_6) 12.23 (1 H, br s, CO_2H), 11.71 (1 H, s, N*H*), 11.15 (1 H, s, N*H*), 8.80 (1 H, d, *J* 1.8, Ar*H*), 8.03–8.00 (1 H, dd, *J* 8.5 and 1.8 , Ar*H*), 8.00–7.97 (1 H, d, *J* 8.2, Ar*H*), 7.97 (1 H, s, Ar*H*), 7.95–7.92 (1 H, d, *J* 8.2, Ar*H*), 7.78–7.74 (1 H, d, *J* 8.5, Ar*H*), 7.60–7.57 (1H, d, *J* 8.2, Ar*H*), 7.24–7.21 (1 H, dd, *J* 8.2 and 1.2, Ar*H*), 2.48 (1 H, s, CH_3); δ_C (125 MHz, DMSO-d_6) 178.4, 172.2, 166.5, 141.8, 137.4, 127.7, 126.3, 126.2, 125.8, 125.6, 123.7, 123.6, 121.8, 120.6,

120.2, 119.9, 119.6, 112.6, 111.5, 111.4, 69.9, 69.8, 68.6, 68.3, 63.7, 63.4, 28.7, 28.6, 21.2; *m*/*z* (ES) 569.1876 ($M + Na^+$, $C_{30}H_{30}N_2NaO_8$ requires 569.1894).

Methyl 2-(2-(2-(8-methyl-11,12-dihydroindolo[2,3-*a*]carbazole-3-carbonyloxy)ethoxy)ethoxy)ethyl succinate 13

1-(8-Methyl-11,12-dihydroindolo[2,3-*a*]carbazol-3-yl)-1,12-dioxo-2,5,8,11-tetraoxapentadecan-15-oic acid **12** (0.060 g, 0.11 mmol) and 4-(dimethylamino)pyridine (0.0030 g, 0.025 mmol) were dissolved in a 1 : 1 v/v mixture of CH_2Cl_2 and MeOH (10 mL) and *N*-(3-dimethylaminopropyl)-*N*′-ethylcarbodiimide hydrochloride (0.084 g, 0.44 mmol) was added. After stirring at room temperature under N_2 for 18 h, the solvent was removed *in vacuo* and the residual yellow solid was purified by column chromatography (SiO_2; 2% MeOH–CH_2Cl_2) to give the product (0.057 g, 93%) as an off-white solid; mp 164–165 °C; δ_H (500 MHz, DMSO-d_6) 11.51 (1 H, s, N*H*), 10.98 (1 H, s, N*H*), 8.80 (1 H. d, *J* 1.5, Ar*H*), 8.02 (1 H, dd, *J* 8.8 and 1.5, Ar*H*), 7.99 (1 H, d, *J* 8.5, Ar*H*), 7.97 (1 H, br s, Ar*H*), 7.93 (1 H, d, *J* 8.5, Ar*H*), 7.77 (1 H, d, *J* 8.5, Ar*H*), 7.59 (1 H, d, *J* 8.2, Ar*H*), 7.23 (1 H, dd, *J* 8.2 and 1.2, Ar*H*), 4.45 (2 H, t, *J* 4.7, CH_2), 4.11 (2 H, t, *J* 4.7, CH_2), 3.82 (2 H, t, *J* .7, CH_2), 3.67–3.57 (10 H, m, CH_2), 3.56 (3 H, s, CH_3); δ_C (125 MHz, DMSO-d_6) 172.3, 171.9, 166.6, 141.8, 137.4, 127.7, 126.4, 126.2, 125.8, 125.6, 123.8, 123.6, 121.8, 120.7, 120.2, 119.9, 119.6, 112.6, 111.5, 111.4, 69.9, 69.8, 68.6, 68.3, 63.7, 63.5, 51.4, 28.5, 28.4, 21.2; *m*/*z* (ES) 583.2029 ($M + Na^+$, $C_{31}H_{31}N_2NaO_8$ requires 583.2051).

TentaGel™-OH bound indolocarbazole 4

1-(8-Methyl-11,12-dihydroindolo[2,3-*a*]carbazol-3-yl)-1,12-dioxo-2,5,8,11-tetraoxapentadecan-15-oic acid **12** (0.148 g, 0.27 mmol), *N*-(3-dimethylaminopropyl)-*N*′-ethylcarbodiimide hydrochloride (0.078 g, 0.41 mmol) and 1-hydroxybenzotriazole hydrate (0.055 g, 0.41 mmol) were dissolved in dry THF (1 mL) and dry CH_2Cl_2 (4 mL). Et_3N (0.042 mL, 0.30 mmol) and TentaGel-OH™ beads (0.030 g, TentaGel™-HL-OH, Sigma Aldrich) were then added and the mixture was allowed to stand at room temperature under N_2 for 10 days without stirring. The beads were then filtered and washed successively with CH_2Cl_2 (5 mL), CH_2Cl_2–MeOH 1 : 1 (5 mL), THF (5 mL), CH_2Cl_2 (5 mL), acetone (5 mL), H_2O (5 mL), 1 M $HCl_{(aq)}$ (5 mL), H_2O (5 mL), sat. $NaHCO_{3(aq)}$ (5 mL), H_2O (5 mL), acetone (5 mL), hexane (2 mL), CH_2Cl_2 (2 mL), hexane (2 mL), CH_2Cl_2 (2 mL), MeOH (4 mL) and diethyl ether (2 mL). The resulting pale yellow beads were dried under high vacuum. Found C 64.36, H 7.88, N 0.58, from which the loading is calculated to be 0.21 mmol g^{-1}; δ_H (400 MHz, CD_3CN) 10.47 (1 H, s, N*H*), 9.98 (1 H, s, N*H*), 8.85 (1 H, s, Ar*H*), 8.07 (1 H, s, Ar*H*), 7.90 (3 H, s, Ar*H*), 7.65 (1 H, d, Ar*H*), 7.49 (1 H, d, Ar*H*), 7.19 (1 H, d, Ar*H*), 4.44 (2 H, br s, CH_2), 4.09 (2 H, m, CH_2), 3.64–3.58 (10 H, m, CH_2).

Acknowledgements

We thank the EPSRC for postdoctoral fellowships (LZ, MJC, KMM), and DTA funding (AB).

References

1 A. R. Pease, J. O. Jeppesen, J. F. Stoddart, Y. Luo, C. P. Collier and J. R. Heath, *Acc. Chem. Res.*, 2001, **34**, 433–444.
2 A. N. Shipway and I. Willner, *Acc. Chem. Res.*, 2001, **34**, 421–432.
3 J. Collin, C. Dietrich-Buchecker, P. Gavin, M. C. Jimenez-Molero and J. Sauvage, *Acc. Chem. Res.*, 2001, **34**, 477–487.
4 J. D. Badjic, V. Balzani, A. Credi, S. Silvi and J. F. Stoddart, *Science*, 2004, **303**, 1845–1849.
5 J. D. Badjic, C. M. Ronconi, J. F. Stoddart, V. Balzani, S. Silvi and A. Credi, *J. Am. Chem. Soc.*, 2005, **128**, 1489–1499.
6 D. S. Marlin, D. G. Cabrera, D. A. Leigh and A. M. Z. Slawin, *Angew. Chem., Int. Ed.*, 2006, **45**, 77–83.
7 D. S. Marlin, D. G. Cabrera, D. A. Leigh and A. M. Z. Slawin, *Angew. Chem., Int. Ed.*, 2006, **45**, 1385–1390.
8 V. Balzani, A. Credi, S. Silvi and M. Venturi, *Chem. Soc. Rev.*, 2006, **35**, 1135–1149.
9 H. Tian and Q.-C. Wang, *Chem. Soc. Rev.*, 2006, **35**, 361–374.
10 D. Tuncel, O. Ozsar, H. B. Tiftik and B. Salih, *Chem. Commun.*, 2007, 1369–1371.
11 E. R. Kay, D. A. Leigh and F. Zerbetto, *Angew. Chem., Int. Ed.*, 2007, **46**, 72–191.
12 P. D. Beer, J. J. Davis, D. A. Drillsma-Milgrom and F. Szemes, *Chem. Commun.*, 2002, 1716–1717.
13 J. J. Davis and P. D. Beer, *The Encyclopedia of Nanoscience and Nanotechnology*, Marcel Dekker, New York, 2004, pp. 2477–2492.
14 S. Chia, J. Cao, J. F. Stoddart and J. I. Zink, *Angew. Chem., Int. Ed.*, 2001, **40**, 2447–2451.
15 F. Cecchet, P. Rudolf, S. Rapino, M. Margotti, F. Paolucci, J. Baggerman, A. M. Brouwer, E. R. Kay, J. K. Y. Wong and D. A. Leigh, *J. Phys. Chem. B*, 2004, **108**, 15192–15199.
16 I. Willner, V. Pardo-Yissar, E. Katz and K. T. Ranjit, *J. Electroanal. Chem.*, 2001, **497**, 172–177.
17 L. Raehm, J.-M. Kern, J.-P. Sauvage, C. Hamann, S. Palacin and J.-P. Bourgoin, *Chem.–Eur. J.*, 2002, **8**, 2153–2162.
18 N. Weber, C. Hamann, J. Kern and J. Sauvage, *Inorg. Chem.*, 2003, **42**, 6780–6792.
19 K. Kim, W. S. Jeon, J.-K. Kang, J. W. Lee, S. Y. Jon, T. Kim and K. Kim, *Angew. Chem., Int. Ed.*, 2003, **42**, 2293–2296.
20 E. Katz, O. Lioubashevsky and I. Willner, *J. Am. Chem. Soc.*, 2004, **126**, 15520–15532.
21 B. Long, K. Nikitin and D. Fitzmaurice, *J. Am. Chem. Soc.*, 2003, **125**, 15490–15498.
22 H. Yu, Y. Luo, K. Beverly, J. F. Stoddart, H.-R. Tseng and J. R. Heath, *Angew. Chem., Int. Ed.*, 2003, **42**, 5706–5711.
23 T. D. Nguyen, K. C.-F. Leung, M. Liong, C. D. Pentecost, J. F. Stoddart and J. I. Zink, *Org. Lett.*, 2006, **8**, 3363–3366.
24 T. D. Nguyen, Y. Liu, S. Saha, K. C. F. Leung, J. F. Stoddart and J. I. Zink, *J. Am. Chem. Soc.*, 2007, **129**, 626–634.
25 M. Clemente-León, A. Credi, M.-V. Martínez-Díaz, C. Mingotaud and J. F. Stoddart, *Adv. Mater.*, 2006, **18**, 1291–1296.
26 S. R. Bayley, T. M. Gray, M. J. Chmielewski, P. D. Beer and J. J. Davis, *Chem. Commun.*, 2007, 2234–2236.
27 M. J. Chmielewski, L. Zhao, A. Brown, D. Curiel, M. R. Sambrook, A. L. Thompson, S. M. Santos, V. Felix, J. J. Davis and P. D. Beer, *Chem. Commun.*, 2008, 3154–3156.
28 K. J. Chang, D. Moon, M. S. Lah and K. S. Jeong, *Angew. Chem., Int. Ed.*, 2005, **44**, 7926–7929.
29 T. H. Kwon and K. S. Jeong, *Tetrahedron Lett.*, 2006, **47**, 8539–8541.
30 K. J. Chang, M. K. Chae, C. Lee, J. Y. Lee and K. S. Jeong, *Tetrahedron Lett.*, 2006, **47**, 6385–6388.
31 J. Y. Lee, M. H. Lee and K. S. Jeong, *Supramol. Chem.*, 2007, **19**, 257–263.
32 K. J. Chang, B. N. Kang, M. H. Lee and K. S. Jeong, *J. Am. Chem. Soc.*, 2005, **127**, 12214–12215.
33 F. M. Pfeffer, K. F. Lim and K. J. Sedgwick, *Org. Biomol. Chem.*, 2007, **5**, 1795–1799.
34 J. L. Sessler, D. G. Cho and V. Lynch, *J. Am. Chem. Soc.*, 2006, **128**, 16518–16519.
35 G. W. Bates, P. A. Gale and M. E. Light, *Chem. Commun.*, 2007, 2121–2123.
36 G. W. Bates, Triyanti, M. E. Light, M. Albrecht and P. A. Gale, *J. Org. Chem.*, 2007, **72**, 8921–8927.

37 D. Curiel, A. Cowley and P. D. Beer, *Chem. Commun.*, 2005, 236–238.
38 P. Piatek, V. M. Lynch and J. L. Sessler, *J. Am. Chem. Soc.*, 2004, **126**, 16073–16076.
39 M. J. Chmielewski, M. Charon and J. Jurczak, *Org. Lett.*, 2004, **6**, 3501–3504.
40 P. A. Gale, *Chem. Commun.*, 2008, 4525–4540.
41 C. Caltagirone, J. R. Hiscock, M. B. Hursthouse, M. E. Light and P. A. Gale, *Chem.–Eur. J.*, 2008, **14**, 10236–10243.
42 C. Caltagirone, P. A. Gale, J. R. Hiscock, S. J. Brooks, M. B. Hursthouse and M. E. Light, *Chem. Commun.*, 2008, 3007–3009.
43 M. D. Lankshear and P. D. Beer, *Acc. Chem. Res.*, 2007, **40**, 657–668.
44 B. J. Egner and M. Bradley, *Drug Discovery Today*, 1997, **2**, 102–109.
45 G. Lippens, M. Bourdonneau, C. Dhalluin, R. Warrass, T. Richert, C. Seetharaman, C. Boutillon and M. Piotto, *Curr. Org. Chem.*, 1999, **3**, 147–169.
46 K. D. Johnstone, N. Bampos, J. K. M. Sanders and M. J. Gunter, *Chem. Commun.*, 2003, 1396–1397.
47 K. D. Johnstone, N. Bampos, J. K. M. Sanders and M. J. Gunter, *New J. Chem.*, 2006, **30**, 861–867.
48 M. J. Shapiro and J. R. Wareing, *Curr. Opin. Chem. Biol.*, 1998, **2**, 372–375.
49 D. Huster, K. Kuhn, D. Kadereit, H. Waldmann and K. Arnold, *Angew. Chem., Int. Ed.*, 2001, **40**, 1056–1058.
50 M. A. Gallop and W. L. Fitch, *Curr. Opin. Chem. Biol.*, 1997, **1**, 94–100.
51 E. Brule, K. K. M. Hii and Y. R. de Miguel, *Org. Biomol. Chem.*, 2005, **3**, 1971–1976.
52 D. Curiel, A. Cowley and P. D. Beer, *Chem. Commun.*, 2005, 236–238.
53 K. M. Mullen, K. D. Johnstone, M. Webb, N. Bampos, J. K. M. Sanders and M. Gunter, *Org. Biomol. Chem.*, 2008, **6**, 278–286.
54 K. D. Johnstone, *Self-Assembling Porphyrin Supramolecules*, PhD Thesis, University of New England, Armidale, 2004.
55 K. Nikitin, B. Long and D. Fitzmaurice, *J. Am. Chem. Soc.*, 2003, **125**, 15490–15498.
56 T. D. Nguyen, H.-R. Tseng, P. C. Celestre, A. H. Flood, Y. Liu, J. F. Stoddart and J. I. Zink, *Proc. Natl. Acad. Sci. U. S. A.*, 2005, **102**, 10029–10034.
57 S. Santra, H. Yang, D. Dutta, J. T. Stanley, P. H. Holloway, W. Tan, B. M. Moudgil and R. A. Mericle, *Chem. Commun.*, 2004, 2810–2812.
58 M. Nakamura, M. Shono and K. Ishimura, *Anal. Chem.*, 2007, **79**, 6507–6514.
59 E. Rampazzo, S. Bonacchi, M. Montalti, L. Prodi and N. Zaccheroni, *J. Am. Chem. Soc.*, 2007, **129**, 14251–14256.
60 E. Rampazzo, E. Brasola, S. Marcuz, F. Mancin, P. Tecilla and U. Tonellato, *J. Mater. Chem.*, 2005, **15**, 2697–2706.
61 G. Farruggia, S. Iotti, L. Prodi, M. Montalti, N. Zaccheroni, P. B. Savage, V. Trapani, P. Sale and F. I. Wolf, *J. Am. Chem. Soc.*, 2006, **128**, 344–350.
62 M. Arduini, F. Mancin, P. Tecilla and U. Tonellato, *Langmuir*, 2007, **23**, 8632–8636.
63 X. Y. Ling, D. N. Reinhoudt and J. Huskens, *Langmuir*, 2006, **22**, 8777–8783.
64 G. Barbillon, A. C. Faure, N. ElKork, P. Moretti, S. Roux, O. Tillement, M. G. Ou, A. Descamps, P. Perriat, A. Vial, J.-L. Bijeon, C. A. Marquette and B. Jacquier, *Nanotechnology*, 2008, **19**, 035705.
65 N. Baker, G. M. Greenway, R. A. Wheatley and C. Wiles, *Analyst*, 2007, **132**, 104–106.
66 K. Patel, S. Angelos, W. R. Dichtel, A. Coskun, Y.-W. Yang, J. I. Zink and J. F. Stoddart, *J. Am. Chem. Soc.*, 2008, **130**, 2382–2383.
67 M. R. Sambrook, P. D. Beer, J. A. Wisner, R. L. Paul, A. R. Cowley, F. Szemes and M. G. B. Drew, *J. Am. Chem. Soc.*, 2005, **127**, 2292–2302.

